

# Structural Features and Magnetic Properties of Co–W Films

V. O. Vas'kovskiy<sup>a, b</sup>, M. N. Volochaev<sup>c</sup>, A. N. Gorkovenko<sup>a</sup>, E. A. Kravtsov<sup>a, b</sup>,  
V. N. Lepalovskiy<sup>a</sup>, and A. A. Feshchenko<sup>a, \*</sup>

<sup>a</sup> Ural Federal University, Yekaterinburg, Russia

<sup>b</sup> Institute of Metal Physics, Ural Branch of Russian Academy of Sciences, Yekaterinburg, Russia

<sup>c</sup> Institute of Physics, Siberian Branch of Russian Academy of Sciences, Krasnoyarsk, Russia

\*e-mail: asynickname@mail.ru

Received March 5, 2021; revised March 5, 2021; accepted March 8, 2021

**Abstract**—The structure and magnetic properties of thin polycrystalline films of  $\text{Co}_{100-x}\text{W}_x$  ( $0 \leq x \leq 30$ ) deposited by magnetron sputtering on glass substrates are investigated including those containing buffer layers of Ta, W, and Ru. It is found that films of pure Co are non-single-phase and contain hcp and fcc crystalline modifications. Doping leads to an increase in the concentration of the fcc phase and an enhancement of the texture of the (111) type, and subsequently to the amorphization of the films. The buffer layers influence to a certain extent on the depth and concentration localization of these transformations. A characteristic feature of the magnetism of Co–W films is a significant perpendicular component in the macroscopic magnetic anisotropy, which leads to a “supercritical” magnetic state. It is shown that its source is the textured fcc phase, the crystalline anisotropy of which is enhanced as a result of doping of cobalt with tungsten.

**Keywords:** film, doping, substrate, structure, magnetic properties

**DOI:** 10.1134/S1063783421070246

## 1. INTRODUCTION

The problem of high-density magnetic recording of information [1–3] stimulates the search for film media with strong magnetic anisotropy including those having a uniaxial nature and orientation of the easy magnetization axis normal to the surface (perpendicular anisotropy). Among the materials potentially suitable in the film state for this role, amorphous alloys of  $3d$  metals with rare earth elements are considered, for example, Tb–Co [4], as well as polycrystalline Co alloys with  $4d$  or  $5d$  transition metals including systems with Mo, W, and Pt [5–8]. In the first case, the perpendicular macroscopic anisotropy is associated with a specific (columnar) inhomogeneity of the microstructure and becomes decisive only near the state of magnetic compensation inherent in ferrimagnetic systems with heavy rare earth elements [9]. The near-compensation region is characterized by low spontaneous magnetization, and in this component the above films are inferior to the second type of film media, in the formation of magnetic anisotropy of which an important role is played by crystalline anisotropy [10]. It is believed that the crystal anisotropy present in Co because of the spin-orbital bond is enhanced by doping due to the hybridization of the energy  $d$ -bands of various transition elements. However, phase separation also occurs in such alloys, and in some cases it may turn out to be the dominant motif in the mechanism of magnetic anisotropy [11].

An integral attribute of the thin-film state of materials is the substrate. Among other things, it has a significant and sometimes decisive influence on the structural-phase state of metal deposits. When glass substrates are used, their structure-forming role can be regulated by additional so-called buffer coatings [12, 13]. This work is devoted to an experimental study of the structural and magnetic properties of films of the Co–W system on glass substrates including those with various buffer coatings.

## 2. METHODOLOGICAL ASPECTS

Films of Co–W alloys were obtained by magnetron sputtering on an Orion-8 setup in the mode of co-sputtering of Co and W targets at a residual gas pressure of  $5 \times 10^{-5}$  Pa and an argon working gas pressure of  $3 \times 10^{-3}$  Pa. Corning cover glasses in their original form or coated with Ta, W, and Ru buffer layers served as substrates. The deposition was carried out under conditions of high-frequency electric bias of the substrates and in the presence of a homogeneous magnetic field (technological field) with strength of 250 Oe in their plane. The W content in the samples was varied in the range of 0–30 at % due to a change in the ratio of the sputtering rates of the corresponding targets. The composition was monitored on a Nano-hunter X-ray fluorescence spectrometer with an error of  $\pm 0.1$  at %. The nominal thicknesses of the buffer

and magnetic layers were 5 and 50 nm, respectively. Structural studies were carried out on an Empyrean diffractometer in  $\text{CoK}\alpha$  radiation and a Hitachi HT7700 TEM transmission electron microscope. To study the magnetic properties and observe the domain structure, an EvicoMagnetics Kerr magnetometer, an NT-MDT NTEGRA-Prima scanning force microscope, and a LakeShore vibromagnetometer were used.

### 3. PRESENTATION AND ANALYSIS OF THE RESULTS

The main task of this work was to elucidate the regularities of structural transformations and the formation of magnetic properties in thin Co–W films in connection with the modification of the surface of the substrates, on which they were deposited, with thickness, as well as under thermal effects. This modification was carried out by application of thin layers of various metals on the surface of the cover glasses. Ta, W or Ru were used for this purpose. All these metals are refractory ones, not prone to diffusion upon contact with other metals, and as buffer layers, one way or another, have been tested as a factor influencing the properties of magnetic films. In particular, Ta is widely used in the production of multilayer magnetic structures with the effect of giant magneto-resistance [14–16]. Despite its own bcc structure, when being in the form of thin practically amorphous layers it promotes the formation of fcc structure and texture of the (111) type in adjacent polycrystalline layers of a number of magnetic metals and alloys. There is information about the use of W as a material for a structure-forming buffer layer. It has a bcc crystal lattice like Ta, but was used to grow pseudo single crystal Gd films with an hcp structure [17]. The hcp structure is inherent in Ru, in contrast to the other two metals, and Ru-containing buffer layers are not attributed to effective factors affecting adjacent layers, at least with an fcc structure [17]. Thus, the presented set of metals for buffer layers met the task of wide variation of the structure-forming properties of the substrates.

#### 3.1. Crystal Structure and Magnetic Properties of Co Films on Various Substrates

The natural state of Co at room temperature corresponds to a hexagonal close-packed (hcp) crystal lattice, the so-called  $\alpha$ -Co, and at temperatures above 700 K it corresponds to a cubic face-centered (fcc) crystal lattice or  $\beta$ -Co. However, in the film state, due to the specificity of the formation of metallic deposits under specific technological conditions including the influence of the substrate, the Co structure may differ from the equilibrium one. In this regard, in order to separate the influence of the factors of the buffer layer and doping, it is advisable to compare the properties of pure Co films on different substrates. The correspond-

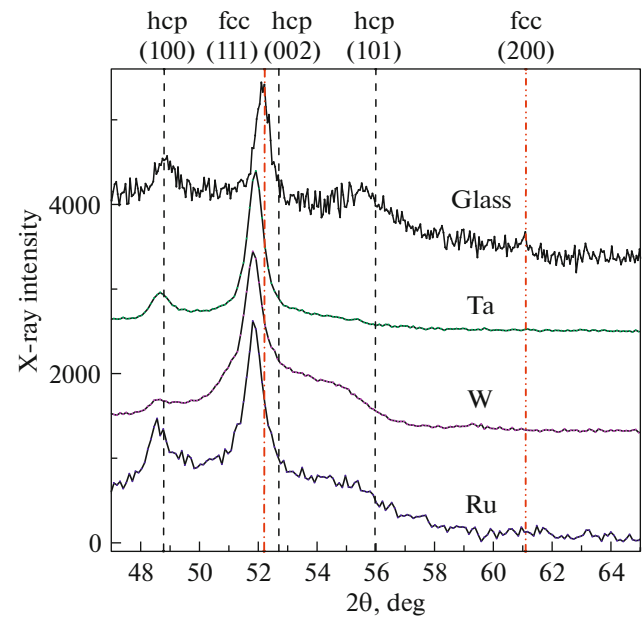


**Fig. 1.** Diffraction patterns of Co films on different substrates. The dotted lines show the position of the diffraction lines of massive  $\alpha$ -Co (hcp) and  $\beta$ -Co (fcc).

ing diffraction patterns in the region of angles containing definitely recorded reflections are shown in Fig. 1. It also shows the positions of the lines of massive Co in two modifications. The presented diffraction pattern indicates a qualitative similarity of films on different substrates, but leaves room for discussion about the structural state of Co itself.

On the one hand, the line near the angle  $2\theta = 49^\circ$ , most likely, belongs to  $\alpha$ -Co and is formed by (100) crystallographic planes. A weakly expressed perturbation observed in diffraction patterns near  $2\theta = 56^\circ$  can be attributed to the same modification, and can be considered as the reflections from the (101) planes. On the other hand, the line near  $2\theta = 52^\circ$  tends to both the (002)  $\alpha$ -Co planes and the (111)  $\beta$ -Co planes, albeit with slightly increased lattice parameters. The latter can be a consequence of residual stresses arising in metal films during their formation on dielectric substrates. We note that the shift of the real line with respect to its corresponding base positions in different modifications will be noticeably less if we attribute it to cubic Co. In addition, the (111) line in the diffraction pattern of isotropic polycrystalline  $\beta$ -Co should have the highest relative intensity. At the same time, for  $\alpha$ -Co, the highest relative intensity is inherent in the (101) line, and the (002) line should be many times weaker. Though, in the case of thin films, the ratio of the intensities of diffraction lines cannot be considered an unambiguous structural criterion, as it distorts when a crystalline texture occurs; this is often observed in films. On the whole, the obtained information leads to the conclusion that the studied films

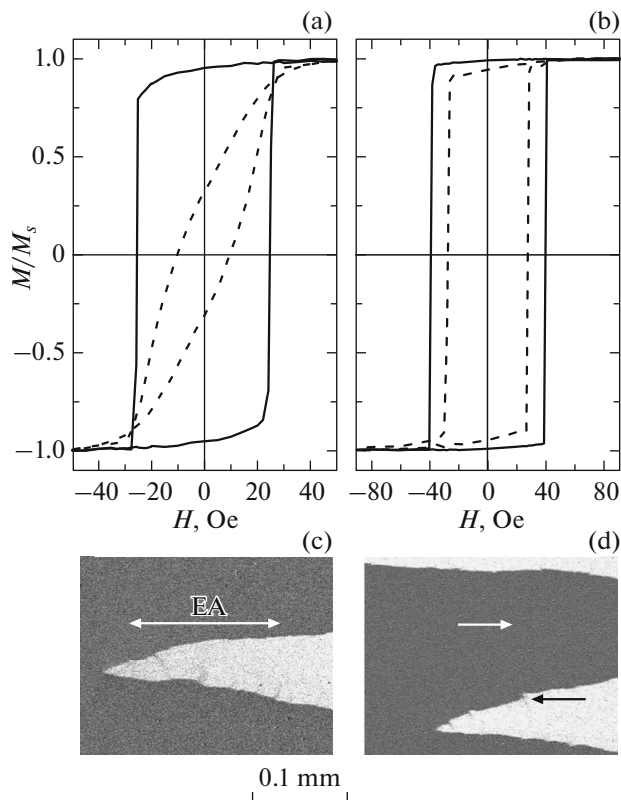


**Fig. 2.** Magneto-optical hysteresis loops measured along (solid curves) and perpendicular (dashed curves) to the axis of the technological field, and images of domains for Co films on (a, c) glass and on (b, d) Ru buffer layer. Double arrow indicates the orientation of the easy magnetization axis (EA), single arrows indicate the orientation of magnetization in domains.

are most likely non-single-phase and contain Co of two modifications. In this case, the presence of buffer coatings plays a secondary role in the formation of the crystal structure itself, but, apparently, has a definite effect on the ratio of volumes of different phases and their texture.

The latter is indirectly confirmed by a significant difference in the hysteresis properties of films on different substrates. This, in particular, can be seen from a comparison of the magneto-optical hysteresis loops of the samples on glass and Ru shown in Figs. 2a and 2b. The first ones demonstrate the presence of pronounced magnetic anisotropy in the plane. This so-called M-induced anisotropy is a typical property of polycrystalline films of  $3d$  metals and their alloys [18]. It is relatively small, has a uniaxial character, and is formed in a state of magnetic saturation, which is provided by a technological magnetic field during the preparation of film samples. The second ones show significantly less anisotropy. In fact, the induced anisotropy is leveled against the background of the large coercive force inherent in these films. However, despite the almost twofold difference in the coercive

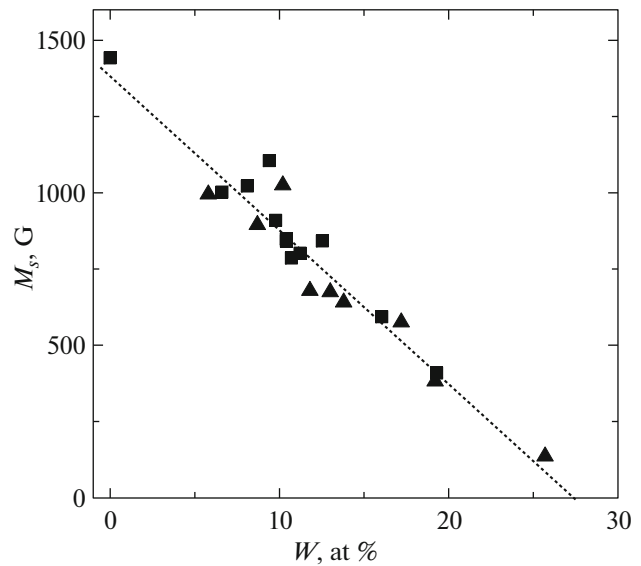


**Fig. 3.** Dependences of spontaneous magnetization on the tungsten content in films of the binary Co–W system deposited on glass (squares) and Ru (triangles).

force, the nature of the magnetization reversal of both types of samples along the easy magnetization axis (EA), which coincides with the axis of application of the technological field, is practically the same. It occurs by abrupt displacement of the zigzag magnetic front (Figs. 2c and 2d). Co films on Ta and W exhibit hysteresis properties close to those of samples on glass and Ru, respectively.

### 3.2. Magnetic Properties of Co–W Films on Various Substrates

The most striking regularities in the change in the magnetic properties of films of the  $\text{Co}_{100-x}\text{W}_x$  binary system are a rapid, close to linear decrease in the spontaneous magnetization with an increase in the W concentration, and a multiple increase in the coercive force, but in a limited range of compositions near  $x \sim 10$ . Figure 3 shows the concentration dependences of the saturation magnetization  $M_s(x)$  by the example of films deposited on glass and on Ru. As can be seen, for samples of two characteristic types, they practically coincide and illustrate the tendency towards a transition to a non-magnetically ordered state at  $x \geq 30$ . Such a sharp drop in magnetization indicates a decrease in the average magnetic moment per Co atom. This, in turn, confirms the concept of a significant modification of the  $3d$  band of the ferromagnet, which occurs due to the  $5d$  electrons of W, and emphasizes its independence from the probable features of the microstructure of films on different substrates.

In contrast to spontaneous magnetization, magnetic hysteresis is a structurally sensitive phenomenon and requires more detailed consideration. Figure 4

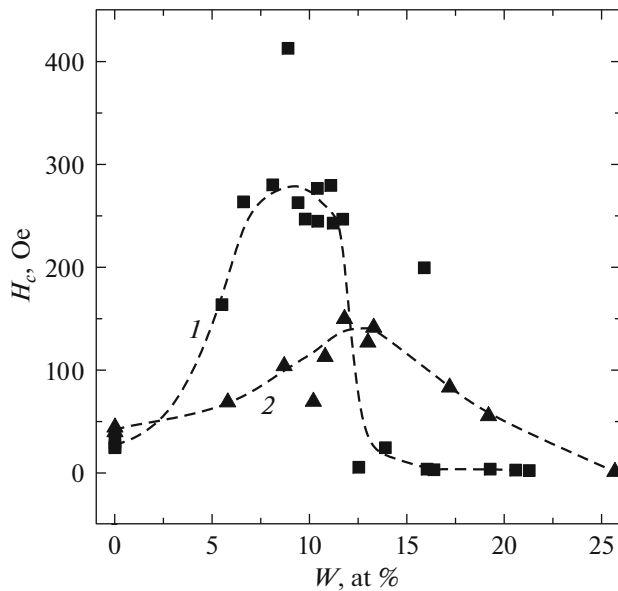


**Fig. 4.** Concentration dependences of the coercive force of  $\text{Co}_{100-x}\text{W}_x$  samples on glass (curve 1) and on Ru (curve 2).

shows the dependences of the coercive force of  $\text{Co}_{100-x}\text{W}_x$  films for the same samples, the values of  $M_s$  of which are shown in Fig. 3. Both  $H_c(x)$  curves are similar in appearance and are characterized by the presence of pronounced maxima. However, in quantitative terms, despite the presence of outliers of the experimental points, we can speak of their significant difference. For films on glass, the maximum values of the coercive force  $H_c$  are, on average, twice as large, and the concentration range of high  $H_c$  is noticeably narrower and is shifted to the region of lower W concentrations. Obviously, the discussion of the reasons for such differences should be preceded by a more detailed analysis of the effect of doping on the hysteresis properties of Co films within the frames of samples of the same type.

Figure 5a shows a magneto-optical loop of a Co–W film on glass containing about 10 at % of a doping element measured along the axis of application of the technological field. Comparison with the corresponding loop for a pure Co film (Fig. 2a) shows that the introduction of W not only increases the coercive force by an order of magnitude, but also changes the shape of the loop itself. Extended inclined sections appear on it, which end in a transition to a state of magnetic saturation in a field exceeding 2 kOe, i.e., two orders of magnitude higher than the saturation field typical for a one-component film. In this case, no magnetic anisotropy is observed in the plane. These features of magnetization reversal are characteristic of the so-called “supercritical” magnetic state [19]. In the absence of an external field, it corresponds to an inhomogeneous magnetic structure of the type of “stripe

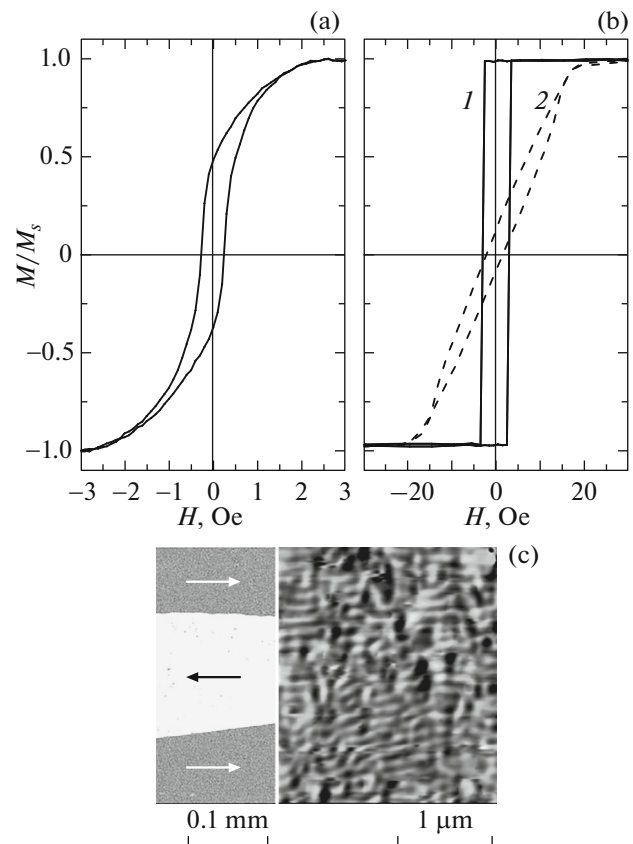


**Fig. 5.** Magneto-optical hysteresis loops of  $\text{Co}_{100-x}\text{W}_x$  films on glass containing (a) 9.8 and (b) 16 at % of W measured along (curves 1) and perpendicular (curve 2) to the axis of the technological field; (c) domain structure revealed by magneto-optical (left) and magneto-force (right) methods in a sample with  $x=9.8$ . The arrows show the orientation of the resulting magnetization in the macro-domains.

domain.” The magnetization in “stripes” is oriented at an angle to the plane of the film so that its planar component in neighboring domains is the same, and the normal component has a different sign.

The magneto-optical image of the domain structure of this sample in the demagnetized state is shown on the left side of Fig. 5c. As can be seen, these are wide stripe domains. However, the magnetic force microscopy shows that these domains have a substructure (Fig. 5c, right-hand side), which is not detected using the Kerr effect due to high dispersion. Thus, we can conclude that the magneto-optical contrast reflects the structure of macro-domains with different orientations of the planar component of magnetization, and the magneto-force one reflects the structure of micro-domains of the “stripe” type. Though, in this case, the “stripe structure” does not differ in the high regularity characteristic of soft magnetic films of the permalloy type [20]. This may be due to the polycrys-

**Table 1.** Typical values of the coercive force of  $\text{Co}_{100-x}\text{W}_x$  films on various substrates

Substrate	$(H_c)_{\max}$ , Oe	$x$	$(H_c)_{\min}$ , Oe	$x$
Glass	412	8.9	2.5	16.4
Ta	451	8.0	2.2	18.5
W	474	13.5	3	24
Ru	149	11.8	0.5	25.7

tallinity and high crystalline anisotropy of the studied objects, as well as to their non-single phase.

As follows from Fig. 4, for samples on glass, the concentration region with high hysteresis is not large. When  $x \sim 13-15$  is reached, the coercive force sharply decreases to a level of several oersteds, i.e., it becomes much less than even those values of  $H_c$  that are inherent in pure Co films. Figure 5b shows magneto-optical loops of one of these samples. They testify about the restoration of uniaxial magnetic anisotropy in the plane of the film and, in general, about the nature of the magnetization reversal inherent in magnetically soft film media. Interestingly that at comparable values of the coercive force, the anisotropy field of Co–W films is much higher than that of permalloy or met-glass films [21].

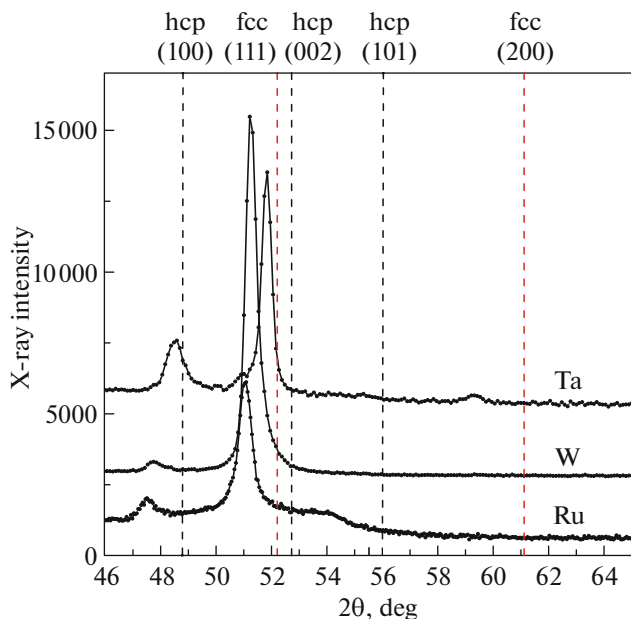
Returning to the discussion of the role of the substrate in the formation of the hysteresis properties of Co–W films, it should be stated that the buffer layers

of Ta and W lead to  $H_c(x)$  dependences similar in character to those shown in Fig. 4. In quantitative terms, they occupy a certain intermediate position. For illustration, Table 1 shows the extreme values of the coercive force and the compositions, at which they were implemented. From its analysis, in particular, it follows that films on Ta in their properties tend to films on glass, and films on W tend to films on Ru. Thus, with a certain similarity in the concentration change in the hysteresis properties of Co–W films of different types, their significant specificity is also evident, which is advisable to associate with the features of the structural state of films on different substrates.

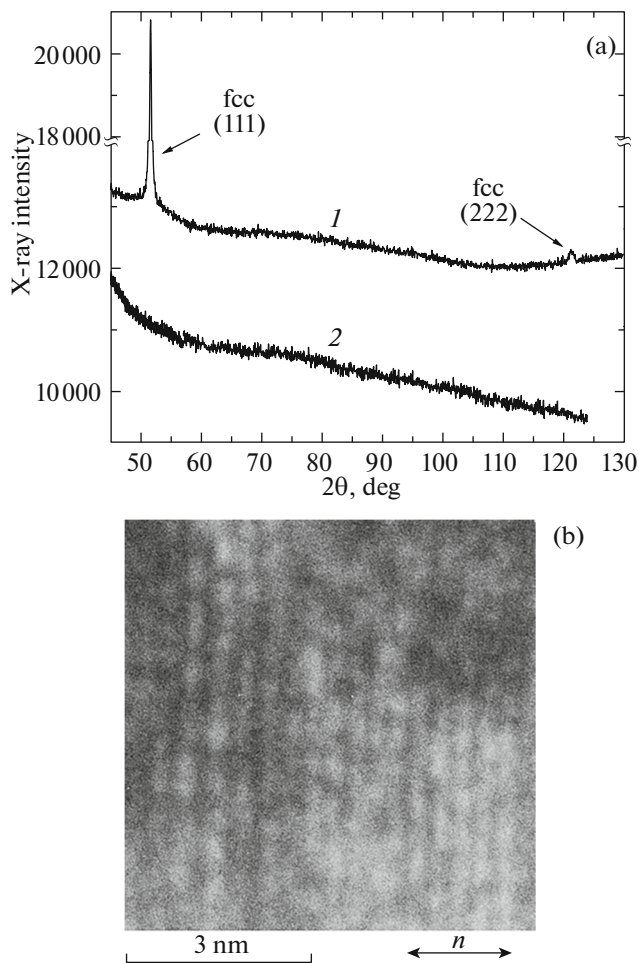
#### 4. CRYSTAL STRUCTURE OF Co–W FILMS ON DIFFERENT SUBSTRATES

Figure 6 shows the diffraction patterns of samples containing metal buffer layers, the composition of which corresponds to the regions of the greatest magnetic hysteresis. Comparing them with similar data for films of pure Co (Fig. 1), we can state the following. The overall diffraction pattern remains unchanged. It still contains lines that can be interpreted as a consequence of the structural two-phase (fcc and hcp phases) of the films. At the same time, a tendency for the lines to shift to the region of smaller diffraction angles can be noted, which indicates the expected increase in interplanar spacings when larger W atoms are introduced into the Co lattice. In addition, there is some change in the ratio of line intensities in favor of the brightest of them, which may indicate redistribution in the volumes of phases and an increase in the crystal texture. Moreover, this feature is more pronounced for films on the W buffer layer and less pronounced on Ru buffer layer.

Films on glass upon doping showed a slightly different change in the structure. As follows from the diffraction pattern shown in Fig. 7a (curve 1), in the region of small diffraction angles, there is only one relatively narrow and high-intensity line. But in the area of large angles of diffraction, a line was clearly defined. Taken together, these lines can be identified as 1st and 2nd orders of reflections from the (111) planes of the fcc crystal lattice under conditions of high crystal texture. The lattice parameter is estimated to be 0.3558 nm, which is comparable to the lattice characteristic of cubic Co (0.3521 nm). The conclusion about the high degree of crystalline texture was also confirmed by the data obtained using high-resolution transmission electron microscopy (TEM). Figure 7b shows a fragment of a TEM image of a cross-section of the film. On it, against the background of spots of different brightness, regularly spaced dark vertical stripes are clearly visible. Regions of irregular contrast can be considered as a mapping of crystallites, and stripes can be considered as a mapping of atomic planes. The closeness of atomic planes in crystallites indicates a sufficiently perfect crystalline texture.



**Fig. 6.** Diffraction patterns of Co–W films on substrates with buffer layers of Ta, W, and Ru, and a tungsten concentration of 8, 13.5, and 13.3 at %, respectively. The dotted lines show the position of the diffraction lines of massive  $\alpha$ -Co (hcp) and  $\beta$ -Co (fcc).



**Fig. 7.** (a) Diffraction patterns and (b) TEM image of Co–W films on substrates without buffer coatings with a W concentration: ((a), curve 1) 10.4, ((a), curve 2) 16, and (b) 11.1 at %. The arrow marked  $n$  shows the orientation of the normal to the film plane.

It should also be noted that weakly pronounced diffraction lines in the region of  $2\theta \sim 120^\circ$  are also recorded on films of other types. This provides additional arguments in favor of associating the brightest line in all the above diffraction patterns with the fcc crystal lattice. Figure 7a also shows an example of a diffraction pattern of a sample with a relatively high content of W. As can be seen, there are no localized diffraction reflections on it at all, which indicates the implementation of an amorphous state. This diffraction pattern refers to  $\text{Co}_{84}\text{W}_{16}$  film on glass. For samples of other types, a similar structural transformation is observed, but the critical concentration of W, at which this occurs, to some extent depends on the presence and composition of the buffer layer. In particular, films on glass and Ta are amorphized at  $x \geq 12\text{--}13$ , and films on W and Ru are amorphized at  $x \geq 15\text{--}20$ .

## 5. CONCLUSIONS

The entire set of the presented results makes it possible to compose a fairly complete picture of the structural features of the Co–W films obtained by magnetron sputtering and to evaluate their influence on the macroscopic magnetic properties. The main factors of this influence are non-single-phase and crystalline texture. In films of pure Co irrespective of the type of substrate crystallites of the hcp and fcc modifications are present. Moreover, at least the latter has a pronounced crystalline texture of the (111) type. However, the relative concentration of these phases can be varied due to the introduction of buffer coatings. Among the tested variants, the hcp phase, which is characterized by uniaxial and rather strong anisotropy (anisotropy constant  $K = 4 \times 10^6 \text{ erg/cm}^3$ ), apparently has a higher concentration in films on W and Ru, thus setting an increased level of magnetic hysteresis. In films on glass and on Ta, the hysteresis is significantly less, which may indicate the predominance of the fcc phase having a weaker four-axis magnetic anisotropy.

The addition of W in a certain concentration range leads to a gradual redistribution of the phase volumes in favor of the fcc component. This structural modification occurs most deeply in samples on glass, which become practically single-phase and highly textured at  $\sim 10$  at % content of W. It is interesting that after this in a narrow concentration range (2–3 at %) the complete destruction of the crystallinity follows. In doped films on Ta and W, the non-single-phase character is retained to a small extent up to the transition to the amorphous state, which, moreover, is stretched over a wider range of compositions. The highest resistance to concentration structural transformations is demonstrated by films on Ru. For them, a significant non-single-phase character remains in the entire region of the crystalline state, and amorphization occurs at a concentration of  $W > 20$  at %.

The concentration changes in the magnetic properties of Co–W films correlate fairly well with the described structural transformations. The most characteristic feature of the magnetism of all types of doped films is the “supercritical” state. As is known [19], it is interpreted as the result of a compromise between the anisotropy of the film shape and the perpendicular magnetic anisotropy of structural origin. As applied to the Co–W system under study, its formation can be considered as evidence of the appearance or enhancement of the perpendicular component of the magnetic anisotropy against the background of a decrease in the contribution from the self-demagnetization effect due to a decrease in spontaneous magnetization. A common structural inhomogeneity responsible for the perpendicular magnetic anisotropy in polycrystalline metal films is the so-called columnar microstructure [22]. However, it was not revealed in the studied objects. In this regard, it is advisable to focus on the crystalline magnetic anisotropy, and not

within the frames of the hcp structure, as, for example, indicated in [23], but in relation to the actually observed fcc structure. In this case, it can be assumed that the enhancement of the perpendicular anisotropy associated with the easy axis of the [111] type upon doping occurs both due to an increase in the texture of the (111) type and due to an increase in the crystalline anisotropy constant. Our estimates show that  $K$  in films on glass reaches values of  $1.5 \times 10^6$  erg/cm<sup>3</sup>, which is atypical for an fcc structure and is comparable to the characteristics of hexagonal Co.

Thus, we associate the “supercritical” magnetic state and high magnetic hysteresis intrinsic in it with the crystal magnetic anisotropy of the fcc phase. It is formed on the basis of the Co fcc lattice and is modified due to the introduction of W. The formation and texturing of such a phase is promoted or hindered by the structure-forming action of the substrate. It is this factor that determines the specificity of the magnetic properties of films deposited on different buffer layers. This, in particular, refers to the differences in the effect of concentration amorphization, which apparently reflects the excess of the solubility limit of W in the fcc structure and is the reason for the implementation of the soft magnetic state in Co–W films.

#### ACKNOWLEDGMENTS

The authors are grateful to A.S. Bolyachkin, M.E. Moskalev, and V.V. Popov for their help in organizing the work and for participating in the discussion of the results.

#### FUNDING

This work was carried out with support by the Ministry of Science and Higher Education of the Russian Federation, topic no. FEUZ-2020-0051.

#### CONFLICT OF INTEREST

The authors declare that they have no conflicts of interest.

#### REFERENCES

1. S. N. Piramanayagam, *J. Appl. Phys.* **102**, 011301 (2007).
2. *Ultra-High-Density Magnetic Recording: Storage Materials and Media Designs*, Ed. by G. Vavaro and F. Casoli (CRC, Boca Raton, 2016).
3. L. Saharan, C. Morrison, Y. Ikeda, K. Takano, J. J. Miles, T. Thomson, T. Schref, and G. Hrkac, *Appl. Phys. Lett.* **102**, 142402 (2013).
4. R. H. Krider, *Ann. Rev. Mater. Sci.* **23**, 411 (1993).
5. K. Oikawa, G. W. Qin, M. Sato, O. Kitakami, and Y. Shimada, *Appl. Phys. Lett.* **83**, 966 (2003).
6. D. Z. Grabco, I. A. Dikusa, V. I. Petrenko, E. E. Harea, and O. A. Shikimaka, *Surf. Eng. Appl. Electrochem.* **43**, 11 (2007).
7. D. A. Dugato, J. Brandão, R. L. Seeger, F. Béron, J. C. Cezar, L. S. Dorneles, and T. J. A. Mori, *Appl. Phys. Lett.* **115**, 182408 (2019).
8. T. R. Gao, Y. Q. Wu, S. Fackler, I. Kierzewski, Y. Zhang, A. Mehta, M. J. Kramer, and I. Takeuchi, *Appl. Phys. Lett.* **102**, 022419 (2013).
9. V. O. Vas'kovskii, A. N. Gor'kovenko, O. A. Adanokova, A. V. Svalov, N. A. Kulesh, E. A. Stepanova, E. V. Kudryukov, and V. N. Lepalovskii, *Phys. Met. Metallogr.* **120**, 1055 (2019).
10. A. Kashyap, P. Manchanda, P. K. Sahota, R. Skomski, J. E. Shield, and D. J. Sellmyer, *IEEE Trans. Magn.* **47**, 3336 (2011).
11. K. Oikawa, G. W. Qin, M. Sato, S. Okamoto, O. Kitakami, and Y. Shimada, *Appl. Phys. Lett.* **85**, 2559 (2003).
12. R. Jérôme, T. Valet, and P. Galtier, *IEEE Trans. Magn.* **30**, 4878 (1994).
13. V. O. Vas'kovskiy, V. N. Lepalovskii, A. N. Gor'kovenko, N. A. Kulesh, P. A. Savin, A. V. Svalov, E. A. Stepanova, N. N. Shchegoleva, and A. A. Yuvchenko, *Tech. Phys.* **60**, 116 (2015).
14. S. Gangopadhyay, J. X. Shen, M. T. Kief, J. A. Barnard, and M. R. Parker, *IEEE Trans. Magn.* **31**, 3933 (1995).
15. R. Coehoorn, in *Handbook of Magnetic Materials*, Ed. by K. H. J. Buschow (North Holland, Amsterdam, 1999).
16. N. S. Bannikova, M. A. Milyaev, L. I. Naumova, E. I. Patrakov, V. V. Proglyado, I. Yu. Kamenskii, M. V. Ryabukhina, and V. V. Ustinov, *Phys. Met. Metallogr.* **119**, 1073 (2018).
17. M. Farle, *Rep. Prog. Phys.* **61**, 755 (1998).
18. A. G. Lesnik, *Induced Magnetic Anisotropy in Polycrystalline Films* (Naukova Dumka, Kiev, 1976) [in Russian].
19. N. M. Salanskii and M. Sh. Erukhimov, *Physical Properties and Applications of Thin Films* (Nauka, Novosibirsk, 1975) [in Russian].
20. V. O. Vas'kovskii, P. A. Savin, S. O. Volchkov, V. N. Lepalovskii, D. A. Bukreev, and A. A. Buchkevich, *Tech. Phys.* **58**, 105 (2013).
21. E. A. Mikhailitsyna, V. A. Kataev, A. Larrañaga, V. N. Lepalovskij, and A. P. Turygin, *J. Magn. Mater.* **415**, 61 (2016).
22. S. R. Herd, *J. Appl. Phys.* **50**, 1645 (1979).
23. S. Q. Yin, Y. Wu, X. G. Xu, H. Wang, J. P. Wang, and Y. Jiang, *AIP Adv.* **4**, 127156 (2014).

*Translated by S. Rostovtseva*